Chaos in cuspy triaxial galaxies with a supermassive black hole: a simple toy model

Henry E. Kandrup (`kandrup@astro.ufl.edu`)
Department of Astronomy, Department of Physics, and Institute for Fundamental Theory, University of Florida, Gainesville, Florida, USA 32611

Ioannis V. Sideris (`sideris@astro.ufl.edu`)
Department of Astronomy, University of Florida, Gainesville, Florida, USA 32611

February 1, 2008

Abstract. This paper summarises an investigation of chaos in a toy potential which mimics much of the behaviour observed for the more realistic triaxial generalisations of the Dehnen potentials, which have been used to model cuspy triaxial galaxies both with and without a supermassive black hole. The potential is the sum of an anisotropic harmonic oscillator potential, $V_o = \frac{1}{2}(a^2 x^2 + b^2 y^2 + c^2 z^2)$, and a spherical Plummer potential, $V_p = -M_{BH}/\sqrt{r^2 + \epsilon^2}$, with $r^2 = x^2 + y^2 + z^2$. Attention focuses on three issues related to the properties of ensembles of chaotic orbits which impact on chaotic mixing and the possibility of constructing self-consistent equilibria: (1) What fraction of the orbits are chaotic? (2) How sensitive are the chaotic orbits, *i.e.*, how large are their largest (short time) Lyapunov exponents? (3) To what extent is the motion of chaotic orbits impeded by Arnold webs, *i.e.*, how 'sticky' are the chaotic orbits? These questions are explored as functions of the axis ratio $a : b : c$, black hole mass M_{BH}, softening length ϵ, and energy E with the aims of understanding how the manifestations of chaos depend on the shape of the system and why the black hole generates chaos. The simplicity of the model makes it amenable to a perturbative analysis. That it mimics the behaviour of more complicated potentials suggests that much of this behaviour should be generic.

Keywords: galaxies: kinematics and dynamics

1. Motivation

Over the past decade it has become apparent that many early-type galaxies are genuinely three-dimensional objects, neither spherical nor axisymmetric (*cf.* Kormendy and Bender 1996) that they typically have a central density cusp (*cf.* Lauer *et al* 1995) and that the center of the galaxy often contains a supermassive black hole (*cf.* Kormendy and Richstone 1995). However, there is substantial numerical evidence (*cf.* Fridman and Merritt 1997) that the combination of triaxiality and a cusp typically yields potentials that admit a large amount of chaos; and there is also evidence indicating that the introduction of a supermassive black hole into a cuspy, triaxial potential causes a further increase in the abundance of chaos (*cf.* Valluri and Merritt 1998). Numerical

explorations indicate further (*cf.* Siopis and Kandrup 2000) that the phase space associated with a cuspy triaxial potential, either with or without a black hole, can be very complex, laced with an intricate Arnold (1964) web that can seriously impede phase space transport, so that chaotic orbits in these potentials can be very 'sticky' in the sense recognised originally by Contopoulos (1971).

However, there are at least two important questions which have not yet been addressed adequately. Why does the combination of triaxiality and a cusp and/or black hole lead to chaos? And to what extent is the observed behaviour generic? Almost all work hitherto has focused on one class of model potentials, namely the triaxial generalisations of the spherical Dehnen (1993) potentials first considered by Merritt and Fridman (1996).

Merritt and Valluri (1996) have argued that a black hole or cusp tends to induce chaos because it serves as a near-singular perturbation that destabilises what would be regular box orbits if the galaxy had a smooth core and there were no black hole. This seems quite reasonable. However, Udry and Pfenniger (1988) have noted a fact well known from nonlinear dynamics (*cf.* Lichtenberg and Lieberman 1992), namely that chaos often arises simply by breaking a symmetry or combining incompatible symmetries. One might therefore argue that a supermassive black hole acts as a source of chaos because of symmetry-breaking: the unperturbed galaxy is triaxial, whereas the perturbation manifests spherical symmetry. This could, *e.g.*, account for the fact that, as a source of chaos, even a comparatively low mass black hole can be more important than a steep cusp. As Valluri and Merritt (1998) noted, 'even a modest black hole, with a mass $\sim 0.3\%$ the mass of the galaxy, is as effective as the steepest central density cusp at inducing stochastic diffusion.' In any event, one knows that a black hole or cusp does not always result in chaos. By carefully maintaining symmetries, one can, *e.g.*, construct integrable generalisations of the Staeckel potentials which incorporate a supermassive black hole (Sridhar and Tousma, 1996; Sridhar and Tousma, 1997).

One objective here is to address the question of why cusps and black holes induce chaos by studying orbits in an extremely simple class of potentials which appear to exhibit behaviour qualitatively similar to what is observed the triaxial Dehnen potentials with or without a black hole. The potential,

$$V(x,y,z) = \frac{1}{2}(a^2x^2 + b^2y^2 + c^2z^2) - \frac{M_{BH}}{\sqrt{r^2 + \epsilon^2}}, \qquad (1)$$

with $r^2 = x^2 + y^2 + z^2$, is the sum of an anisotropic harmonic potential and a spherical Plummer potential. There are five parameters which

can be varied independently, namely a, b, and c, which determine the frequencies and the shape of the unperturbed oscillator, M_{BH}, the mass of the black hole, and the softening length ϵ. That much of the behaviour exhibited by orbits in the triaxial Dehnen potentials can be reproduced by such a simple model suggests that it may be generic. That the model is so simple implies that it is amenable to an analytic treatment with the black hole viewed as a perturbation of the integrable oscillator potential.

The numerical component of the analysis focuses on three important characterisations of the chaos: (1) What fraction of the orbits are chaotic? (2) How large is the largest Lyapunov exponent associated with the chaotic orbits? (3) How 'sticky' are the chaotic orbits? Can they travel relatively unimpeded throughout the accessible phase space, or is their motion obstructed significantly by the Arnold web?

The relative abundance of chaotic orbits is important given the general presumption that one requires a substantial number of regular, or nearly regular, orbits to serve as a skeleton for the equilibrium (*cf.* Binney 1978). The degree of sensitivity exhibited by orbits is important because it impacts on the efficacy of chaotic mixing (*cf.* Kandrup and Mahon 1994, Merritt and Valluri 1999). The existence of "sticky" orbits is of potential importance because these orbits can in principal be used to support regular structures in phase space regions where few, if any, regular orbits exist (*cf.* Wozniak 1993, Kaufmann and Contopoulos 1996, Patsis, Athanassoula, and Quillen 1997).

Determining the answers to these questions as functions of the axis ratio $a : b : c$ and the black hole mass M_{BH} provides information about how the manifestations of chaos vary with the degree of triaxiality and the mass of the black hole. Determining the effects of varying ϵ can shed insights into why the chaos arises. For sufficiently small softening, the exact value of ϵ is immaterial, but when ϵ becomes too large its value begins to have an important effect.

If the only function of the black hole were to act as a near-singular perturbation, one might expect that, for ensembles of orbits with fixed energy E, unperturbed frequencies a, b, and c, and softening ϵ, the relative abundance of chaotic orbits should exhibit a very simple dependence on M_{BH}. For $M_{BH} = 0$ and $M_{BH} \to \infty$ the potential is integrable. However, for other values V is nonintegrable and, for intermediate values far from $M_{BH} = 0$ and ∞, one might expect large measures of chaotic orbits. In particular, one might expect that a plot of $n(M_{BH})$, the relative measure of chaotic orbits, as a function of M_{BH} would exhibit a single maximum at an intermediate value where M_{BH} is neither too small nor too large. This is *not* what the numerical simulations reveal. Rather, one finds that the abundance of chaos varies

in a more irregular fashion which, as discussed in Section 2, would suggest that chaos arises from a resonance overlap between the natural frequencies of the oscillator and the black hole.

Section 2 of this paper focuses on the statistical properties of short time Lyapunov exponents. Section 3 summarises an analysis that focused primarily on the Fourier spectra of both individual orbits and orbit ensembles. Section 4 concludes by summarising the results of Sections 2 and 3 and commenting on their physical implications.

2. Lyapunov Exponents for Orbit Ensembles

2.1. WHAT WAS COMPUTED

Most of the experiments focused on the statistical properties of ensembles of orbits evolved for comparatively short times. However, these were supplemented by very long time integrations of individual initial conditions used to extract estimates of the values of the largest Lyapunov exponents for fixed values of frequencies a, b, c, mass M_{BH}, softening ϵ, and energy E. Three different questions were addressed:

1. For fixed a, b, c, M_{BH}, and E, how do things depend on ϵ? For sufficiently small ϵ, the precise value is immaterial but for larger ϵ this is no longer true.

2. For fixed a, b, c, ϵ, and E, how do things depend on M_{BH}? The most naive picture might suggest that $n(M_{BH})$, the relative measure of chaotic orbits, should vary smoothly with M_{BH} and that a plot of n as a function of M_{BH} should exhibit no structure.

3. For fixed ϵ, M_{BH}, and E, how do things depend on the axis ratio $a : b : c$? Conventional wisdom would suggest that larger deviations from spherical symmetry imply more chaos, so that one might expect the relative abundance of chaos to increase monotonically with increasing asphericity.

The experiments were performed for frequencies a, b, and $c \sim 1$ and energies $E \sim 0.1 - 1$, this corresponding physically to a galaxy of mass $M \sim 1$, linear size $r \sim 1$, and characteristical orbital, or dynamical, time scale $t_D \sim 2 - 3$. The black hole mass was taken in the range $10^{-4} \leq M_{BH} \leq 1$. Smaller black hole masses are not large enough to induce significant stochasticity; much larger masses seem completely unrealistic.

For parameters in these general ranges, the exact value of ϵ seems unimportant, provided only that $\epsilon^2 < 10^{-3}$ or so. For this reason, most of the experiments were performed assuming $\epsilon^2 = 10^{-4}$, the same value used in Siopis & Kandrup (2000). A 'typical' choice of frequencies was

$a^2 = 1.25$, $b^2 = 1.0$, and $c^2 = 0.75$, corresponding to a moderately triaxial configuration.

For fixed frequencies a, b and c, mass M_{BH}, and energy E, the value of the largest Lyapunov exponent was estimated by selecting six or more initial conditions corresponding to chaotic orbits and integrating each initial condition for a total time $t = 256000$ while simultaneously tracking the evolution of a small initial perturbation periodically renormalised in the usual way (*cf.* Lichtenberg and Lieberman 1992). The relative abundance of chaotic orbits was estimated by sampling the phase space to generate a collection of 2000 initial conditions and evolving each of these initial conditions, along with a small perturbation, for a time $t = 2048$ which, for the energies considered here, corresponded to $\sim 800 t_D$. The value of the largest short time Lyapunov exponent χ (*cf.* Grassberger *et al* 1988) was then used as a diagnostic to determine whether or not the initial condition was chaotic. (Integrations for shorter times would seem better motivated astronomically, but it was found that, for much smaller t, it was often impossible to determine with any reliability whether or not any given segment corresponded to a chaotic orbit. Indeed, even for integrations for times as long as $t = 2048$ it is possible that some very sticky chaotic segments were misinterpreted as regular segments!) The initial conditions were generated as in Siopis and Kandrup (2000), using a scheme which generalises Schwarzschild's (1993) algorithm to construct a representative library of orbits.

The resulting short time χ's were examined to determine three things, namely (1) the relative number of chaotic orbits; (2) the degree to which different chaotic orbit segments with the same energy do, or do not, have the same short time χ's, and (3) the degree to which all the chaotic segments are characterised by short time χ's well separated from zero. The behaviour of orbit segments over shorter, more astronomically relevant, time scales was addressed by partitioning each of the 2000 segments of length $t = 2048$ into eight segments of length $t = 256$ and extracting a short time Lyapunov exponent for each segment (*cf.* Kandrup and Mahon 1994). The resulting 16000 segments were analysed to determine a distribution of short time Lyapunov exponents, $N[\chi(t = 256)]$, which probes the varying degrees of chaos exhibited by a representative collection of orbits, both regular and chaotic, over an interval of time comparable to the age of the Universe. Finally, as another probe of the total amount of chaos, independent of distinctions amongst regular, sticky, and wildly chaotic orbits, the output was analysed to extract the average short time Lyapunov exponent for *all* the orbits in each ensemble.

Most of the experiments focused on three representative energies, $E = 1.0$, 0.6, and 0.4. A variety of axis ratios were considered. One set of experiments involved considering frequencies a, b, and c for which $a^2 : b^2 : c^2 = 1 + \Delta : 1 : 1 - \Delta$ and exploring the effects of increasing Δ.

2.2. WHAT WAS FOUND

The black hole acts as an important source of chaos whenever conditions are such that the force that it exerts on a test particle often becomes comparable to the force associated with the oscillator. For small ϵ, a mass $M_{BH} > M_{min} \sim 10^{-3}$ appears required to induce an appreciable amount of obvious chaos. The precise value of ϵ seems unimportant provided only that ϵ is very small compared with the characteristic size of a stellar orbit. If the black hole mass be frozen at some value M_{BH} significantly above M_{min} and ϵ increased systematically, chaos remains common until the maximum black hole force $\sim M_{BH}/\epsilon^2$ becomes smaller than a characteristic value somewhat less than unity, this corresponding to the typical force exerted by the oscillator. It thus appears that it is not the singular character of the perturbation *per se* that is responsible for triggering chaos; rather what is important is that the force associated with the black hole can become comparable to, or larger than, the force associated with the unperturbed oscillator. In other words, mixing two integrable potentials of comparable strength is responsible for the chaos.

One example of how the amount of chaos depends on ϵ is provided by Figure 1, each panel of which exhibits the computed short time $\chi(t = 2048)$ for a collection of 2000 initial conditions evolved in the potential (1) with $a^2 = 1.25$, $b^2 = 1.0$, $c^2 = 0.75$, and $M_{BH} = 0.1$ with fixed energy $E = 1.0$. Each panel was constructed by computing 2000 short time χ's, ordering the orbits in terms of the computed χ, and then (*cf.* Siopis and Kandrup 2000) plotting the resulting χ's as a function of particle number from 1 to 2000. The six panels exhibit data for values of ϵ ranging from $\epsilon^2 = 10^{-1}$ to 10^{-6}. The computed χ's for $\epsilon^2 = 10^{-3}$, 10^{-4}, and 10^{-5} are virtually identical. For $\epsilon^2 = 10^{-2}$ chaos is weaker in two senses, namely that the relative number of chaotic orbits is smaller *and* that the typical χ associated with a chaotic orbit has also decreased. For $\epsilon^2 = 10^{-1}$, chaos is almost completely suppressed. For $\epsilon^2 = 10^{-6}$, there are a few orbits with somewhat larger χ's than was observed for $\epsilon^2 = 10^{-5}$, 10^{-4}, and 10^{-3}, each corresponding to a particle which passed extremely close to the black hole.

Overall, chaotic orbits tend to be extremely sticky. In particular, even for $t = 800t_D$ or larger, the computed values of χ need not man-
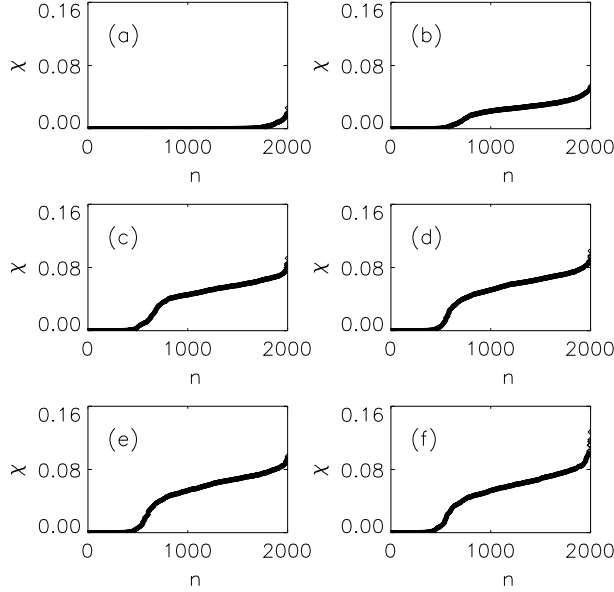
Figure 1. Short time $\chi(t = 2048)$ for 2000 orbits evolved in the potential (1) with $a^2 = 1.25$, $b^2 = 1.0$, $c^2 = 0.75$, $E = 1.0$, and $M_{BH} = 0.1$ with variable ϵ. (a) $\epsilon = 10^{-0.5}$. (b) $\epsilon = 10^{-1.0}$. (c) $\epsilon = 10^{-1.5}$. (d) $\epsilon = 10^{-2.0}$. (e) $\epsilon = 10^{-2.5}$. (f) $\epsilon = 10^{-3.0}$.

ifest a clear and unambiguous separation between regular and chaotic behaviour. If, as in Figure 1, an ordered list of χ's is plotted as a function of particle number, there is in general no clean break between the regular and chaotic orbits. Oftentimes the only way to infer a reasonable demarcation between regular and chaotic behaviour is to look for a 'kink' in the slope. However, the relative abundance of regular/nearly regular as opposed to wildly chaotic orbits *can* be extracted by examining distributions of short time Lyapunov exponents, $N[\chi(t)]$. Typical examples of such distributions are provided in Figures 2 and 3, which exhibit $N[\chi(t)]$ for $t = 256$ and $t = 2048$ for the 2000 orbit ensembles evolved with $a^2 = 1.25$, $b^2 = 1.0$, $c^2 = 0.75$, $\epsilon = 10^{-2}$, and $E = 1.0$ with variable black hole masses ranging between $M_{BH} = 10^{-3.5}$ and $M_{BH} = 1$.

In each of these panels, the data were so plotted that the horizontal axis terminates at the right at a value χ_{max} corresponding to the largest value of $\chi(t = 256)$ assumed by any of the 16000 segments. It is thus evident that, for small M_{BH}, there are a very few orbits with comparatively large values of χ, even though the overwhelming majority of the orbits have much smaller values. For relatively large values of M_{BH}, *e.g.*, $M_{BH} = 10^{-0.25}$, there are comparable numbers
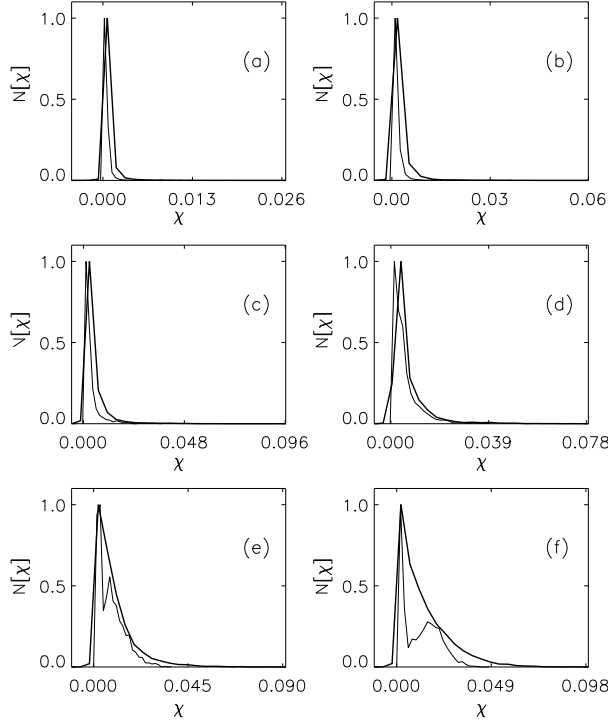
Figure 2. Distribution of short time Lyapunov exponents, $N[\chi(t = 256)]$ (thick lines) and $N[\chi(t = 2048)]$ (thin lines) generated from 2000 orbit segments evolved in the potential (1) with $a^2 = 1.0$, $b^2 = 1.25$, $c^2 = 0.75$, $E = 1.0$, $\epsilon = 10^{-2}$, and variable M_{BH}. (a) $\log_{10} M_{BH} = -3.5$. (b) $\log_{10} M_{BH} = -3.0$. (c) $\log_{10} M_{BH} = -2.5$.(d) $\log_{10} M_{BH} = -2.25$. (e) $\log_{10} M_{BH} = -2.0$. (f) $\log_{10} M_{BH} = -1.75$.

of both regular/nearly regular and wildly chaotic orbits. For somewhat lower values, the abundance of wildly chaotic orbits tends to decrease with increasing M_{BH}, although the trend is not completely uniform. Thus, *e.g.*, there are more wildly chaotic orbits for $M_{BH} = 10^{-0.5}$ and $M_{BH} = 10^{-1.5}$ than for $M_{BH} = 10^{-1}$.

For small values of M_{BH}, it becomes exceedingly difficult to estimate the fraction of the orbits which are truly chaotic. In particular, for $M_{BH} = 10^{-2}$ and less, the distribution $N[\chi]$ manifests a single sharp peak at a value close to zero. This might suggest that the orbits are all regular; but $N[\chi]$ also has a tail extending to much larger values which is clearly indicative of chaos. One possible interpretation is that, *for small M_{BH}, many/all of the orbits are in fact chaotic, but that most of these chaotic orbits behave in a near-regular fashion almost all of the time.* For $M_{BH} = 0$, each initial condition corresponds to a regular box orbit which densely fills a region in configuration space that includes
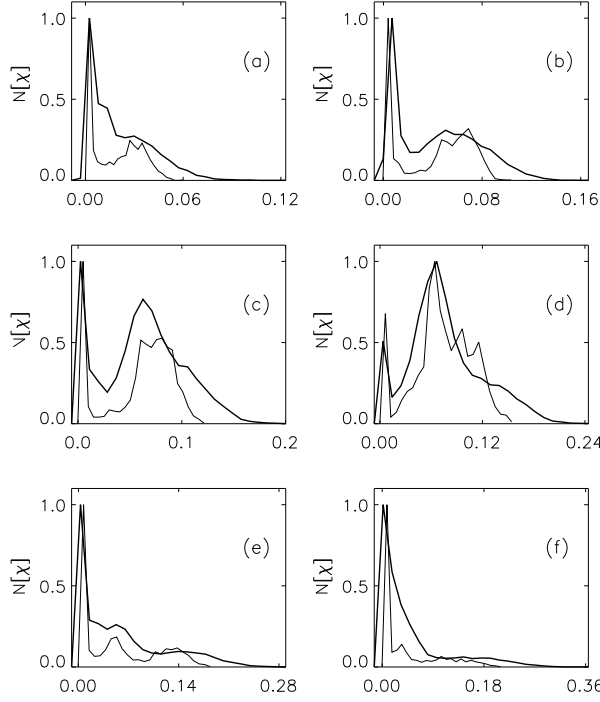
Figure 3. Distribution of short time Lyapunov exponents, $N[\chi(t = 256)]$ (thick lines) and $N[\chi(t = 2048)]$ (thin lines) generated from 2000 orbit segments evolved in the potential (1) with $a^2 = 1.0$, $b^2 = 1.25$, $c^2 = 0.75$, $E = 1.0$, $\epsilon = 10^{-2}$, and variable M_{BH}. (a) $\log_{10} M_{BH} = -1.5$. (b) $\log_{10} M_{BH} = -1.0$. (c) $\log_{10} M_{BH} = -0.75$. (d) $\log_{10} M_{BH} = -0.5$. (e) $\log_{10} M_{BH} = -0.25$. (f) $\log_{10} M_{BH} = 0$.

the origin. One might perhaps expect that, for sufficiently small M_{BH}, the orbits remain "nearly boxy" and again follow trajectories which occasionally bring them arbitrarily close to the origin. In the limit $\epsilon \to 0$, one would thus anticipate that every orbit eventually experiences perturbations of arbitrarily large amplitude which trigger chaotic behaviour. Making ϵ finite introduces a bound to the perturbing force but, for ϵ as small as 10^{-2}, the value used here, this still corresponds to a maximum force of amplitude $10^4 M_{BH}$.

This interpretation is corroborated by the fact that similar distributions of short time Lyapunov exponents can be generated from a single initial condition integrated for very long times. Specifically, if a single initial condition with the same energy be integrated for a time $k \times 256$ and short time exponents computed separately for each $t = 256$ segment, the resulting $N[\chi]$ is often nearly indistinguishable from the $N[\chi]$ generated from an ensemble of initial conditions. This is, *e.g.*,
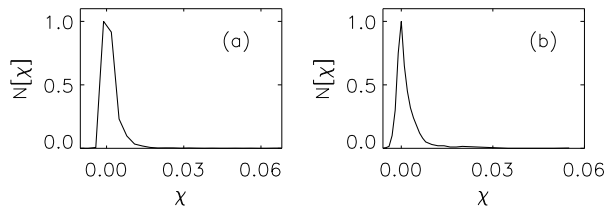
Figure 4. (a) Distribution of short time Lyapunov exponents, $N[\chi(t = 256)]$ generated from a single initial condition with $a^2 = 1.0$, $b^2 = 1.25$, $c^2 = 0.75$, $\epsilon = 10^{-2}$, $E = 1.0$, and $M_{BH} = 10^{-3}$ integrated for a total time $t = 8000 \times 256$. The initial condition corresponded to an orbit which for early times was wildly chaotic. (b) $N[\chi(t = 256)]$ for another initial condition with the same parameter values, in this case corresponding at early times to a 'sticky,' near-regular orbit.

evident from Figure 4, which exhibits distributions generated for two different initial conditions with $E = 1.0$ integrated with $a^2 = 1.25$, $b^2 = 1.0$, $c^2 = 0.75$, $\epsilon = 10^{-2}$, and $M_{BH} = 10^{-3}$. Each initial condition was integrated for a total time $t = 8000 \times 256$ with energy conserved to better than one part in 10^6. One corresponded at early times to a wildly chaotic orbit with $\chi(t = 256) \approx 0.06$; the other corresponded initially to a very 'sticky,' near-regular orbit.

Figure 5 exhibits estimates of χ, the largest Lyapunov exponent, and $n(M_{BH})$, the relative fraction of obviously chaotic orbits, as functions of M_{BH} for representative ensembles computed with $a^2 = 1.25$, $b^2 = 1.0$, $c^2 = 0.75$, and $\epsilon = 10^{-2}$ for three different energies, namely $E = 1.0$, $E = 0.6$, and $E = 0.4$. Only the data for $M_{BH} \geq 10^{-2.5}$ are exhibited since, as noted above, for smaller values it becomes extremely difficult to determine whether any given orbit is regular or chaotic. However, it *does* seem clear that there is little or no chaos when the black hole mass is as small as $M_{BH} = 10^{-4}$, and that there is a comparatively rapid increase in the importance of chaos for $M_{BH} \sim 10^{-3}$. This rapid increase is probably not generic. Rather, as discussed in Section 4, the fact that chaos appears to 'turn on' abruptly likely reflects the fact that, for this potential, all the unperturbed ($M_{BH} = 0$) orbits with fixed energy E have exactly the same natural frequencies and densely sample the same region in configuration space, so that 'if you've seen one orbit you've seen them all.'

If the black hole mass be increased from $M_{BH} = 10^{-2.5}$ to larger values, the overall abundance of chaos tends to decrease. However, this decrease is *not* completely uniform. For all three energies, one observes a pronounced spike in the distribution $n(M_{BH})$ where the relative measure of chaotic orbits increases abruptly. The existence of these
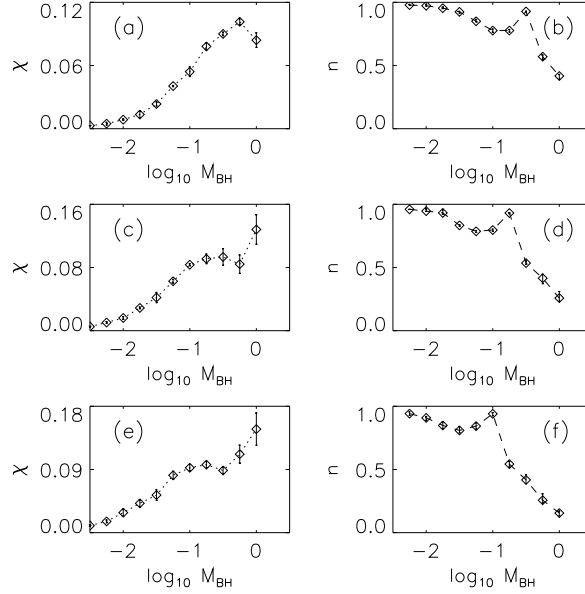
Figure 5. (a) Estimates of the largest Lyapunov exponent for chaotic orbits evolved in the potential with $a^2 = 1.0$, $b^2 = 1.25$, $c^2 = 0.75$, $\epsilon = 10^{-2}$, and $E = 1.0$ as a function of M_{BH}. (b) The fraction of chaotic orbits from a representative ensemble with the same a, b, c, ϵ, and E as a function of M_{BH}. (c) and (d) The same as (a) and (b) but for $E = 0.6$. (e) and (f) The same as (a) and (b) for $E = 0.4$.

spikes indicates that the relative abundance of chaos does not exhibit a completely trivial dependence on M_{BH}. The fact that the locations of these spikes varies smoothly with energy suggests strongly that this nontrivial variation is a resonance phenomenon.

Similarly, for fixed a, b, c, ϵ, and E, the largest Lyapunov exponent, as defined in an asymptotic $t \to \infty$ limit, does not exhibit a completely trivial dependence on M_{BH}. In particular, χ is not a monotonically increasing function of M_{BH}. However, for ensembles integrated for times $t \sim 100 - 800 t_D$, it appears that the largest short time exponents observed for any of the orbits *do* increase monotonically with increasing M_{BH}. The fact that, for certain ranges of M_{BH}, the asymptotic χ decreases reflects the fact that, for these values of M_{BH}, it is especially likely for a chaotic orbit to be 'nearly regular' for long times, during which the short time χ is comparatively small. That the locations of these 'dips' varies smoothly with energy again suggests that some resonance phenomenon has come into play.

Overall, chaos seems to become more pronounced for larger deviations from axisymmetry but, once again, the trend is not completely uniform. Rather, it is again possible to observe dips and/or spikes in the
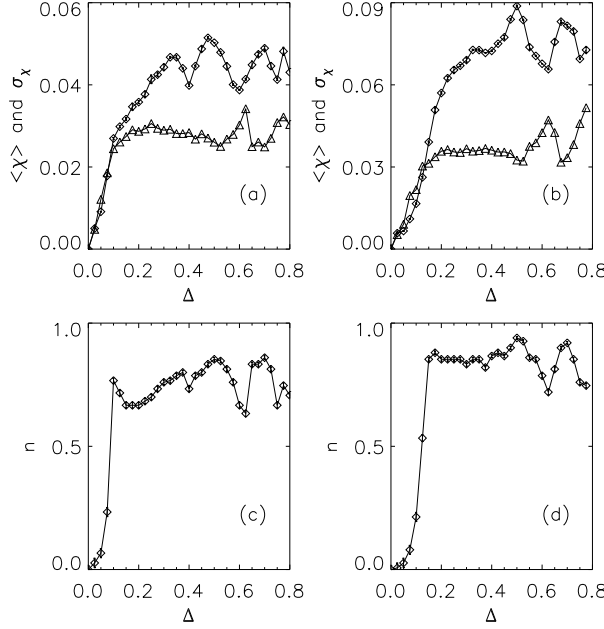
Figure 6. (a) The average short time Lyapunov exponents, $\langle \chi \rangle$ (diamonds), and the associated dispersions, σ_χ (triangles), for representative ensembles with $\epsilon = 10^{-2}$, $E = 1.0$, $M_{BH} = 0.1$, and $a^2 : b^2 : c^2 = 1 + \Delta : 1 : 1 - \Delta$ for variable Δ. (b) The same for an ensemble with $E = 0.6$. (c) The fraction n of wildly chaotic orbits for the $E = 1.0$ ensemble in (a). (d) The same for the $E = 0.6$ ensemble.

relative measure of chaotic orbits. This is, *e.g.*, illustrated by Figure 6, which exhibits $\langle \chi \rangle$, the mean value of the largest Lyapunov exponent, σ_χ, the associated dispersion, and n, the relative abundance of strongly chaotic orbits for sequences of models with fixed E, $M_{BH} = 0.1$, $\epsilon = 10^{-2}$, and $a^2 : b^2 : c^2 = 1 + \Delta : 1 : 1 - \Delta$ with $0 \leq \Delta \leq 0.8$. The two left panels were computed for ensembles with $E = 1.0$; the two right panels were computed for $E = 0.6$.

3. Spectral Properties of Orbits and Orbit Ensembles

3.1. WHAT WAS COMPUTED

The experiments described here aimed to provide additional insights into the origins of chaos in the potential (1) by examining the Fourier spectra of representative orbits and orbit ensembles; testing the validity of a perturbative analysis which views $V_p = -M_{BH}/\sqrt{r^2 + \epsilon^2}$ as a

perturbation of the unperturbed oscillator potential; and examining how, for individual orbits, the degree of instability exhibited at different points correlates with the location of the orbit in configuration space.

Two classes of experiments were considered. The first involved computing Fourier spectra for each orbit in several of the ensembles described in the preceding section. This facilitated an improved understanding of how various orbits with the same E, a, b, c, ϵ, and M_{BH} can differ one from another.

The other class of experiments explored the question of how, for a fixed set of initial conditions, evolved with the same choices of a, b, c, and ϵ, varying the central mass M_{BH} impacts bulk statistical properties. This entailed selecting fifty representative phase space points, uniformly sampling the interval $0.16 < r < 1.4$, with $v_y = v_z = 0$ and v_x so chosen that $E = 1.0$ for $M_{BH} = 0.1$; and then evolving these into the future for a time $t = 2048$ with $a^2 = 1.25$, $b^2 = 1.0$, $c^2 = 0.75$, and $\epsilon = 10^{-2}$, varying the black hole mass incrementally from $M_{BH} = 0$ to $M_{BH} = 0.4$ in steps of 0.01. An analysis of the resulting Fourier spectra facilitated a quantitative characterisation of the extent to which perturbation theory correctly predicts changes in frequencies. A comparison of short time Lyapunov exponents and properties of the Fourier spectra for the orbits corroborated the expectation that, as for other two- and three-dimensional potentials (*cf.* Kandrup *et al* 1997, Siopis *et al* 1998), orbit segments with larger Lyapunov exponents typically have more 'complex' Fourier spectra, with substantial power at a larger number of different frequencies.

The notion of 'complexity' exploited here differs slightly from that adopted in earlier papers. In those papers, the complexity $n(k)$ was defined as the number of frequencies required in a discrete Fourier spectrum to capture a fixed fraction k of the total power. Here the complexity was defined instead as equaling the number of frequencies which contained power greater than or equal to a fixed fraction k of the power at the peak frequency. The results exhibited here involved the choice $k = 0.7$ and a complexity

$$n(\omega) = \frac{1}{3} \left[n_x(\omega) + n_y(\omega) + n_x(\omega) \right] \tag{2}$$

where, *e.g.*, n_x denotes the number of frequencies for motion in the x-direction. The alternative prescription exploited here reflects the fact that there is no obvious unique definition of complexity, and that different definitions yield comparable results.

The analytic computation of modified frequencies was effected using standard second order perturbation theory (*cf.* Lichtenberg and Lieberman 1992). Relevant formulae are summarised in an Appendix.
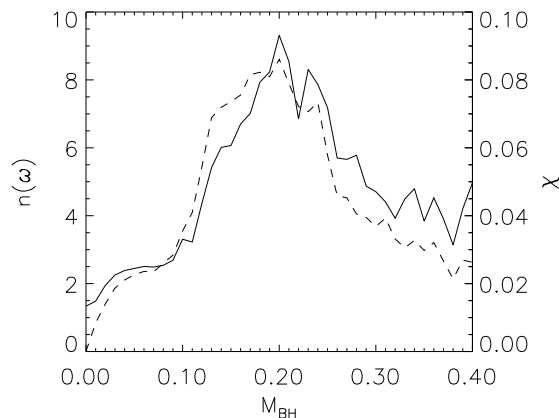
Figure 7. $n(\omega)$, the mean number of frequencies with amplitude greater than 0.7 times the frequency with peak power (solid curve), and χ, the mean short time Lyapunov exponent (dashed curve), computed for the same set of fifty different initial conditions with $E = 1.0$ evolved in the potential (1) for $t = 2048$ with $a^2 = 1.25$, $b^2 = 1.0$, and $c^2 = 0.75$, for a range of black hole masses $0 \leq M_{BH} \leq 0.4$.

3.2. WHAT WAS FOUND

Overall, the complexities of different orbit segments correlate well with the values of the largest short time Lyapunov exponent χ: orbits for which power is spread over a larger number of frequencies tend systematically to have larger values of χ. That this should be the case for different orbits evolved in the same potential with the same energy is hardly surprising, given results for other three-dimensional potentials (*cf.* Siopis *et al* 1998). Less obvious, however, but also true is that such a correlation persists even when comparing ensembles with different values of M_{BH}. This is, *e.g.*, evident from Figure 7, which plots as a function of M_{BH} the average values of $n(\omega)$ (solid curve) and χ (dashed curve) for the aforementioned fifty orbit ensembles. It is clear that the two plots are quite similar, each peaking at a mass $M_{BH} \sim 0.2$ where, consistent with Figures 2 and 3, the relative measure of wildly chaotic orbits is especially high.

For most values of M_{BH} there are relatively few orbits with very large values of χ: most of the orbits are either regular or nearly regular. For example, for $E = 1.0$, $a^2 = 1.25$, $b^2 = 1.0$, and $c^2 = 0.75$, there are large measures of wildly chaotic orbits only for M_{BH} between about $10^{-1.5}$ and $10^{-0.5}$. For much larger or smaller values M_{BH} one finds that $N[\chi]$, the distribution of short time Lyapunov exponents, is a decreasing function of χ. Thus, it is hardly surprising that $N[n]$, the distribution of complexities, should be a decreasing function of n.
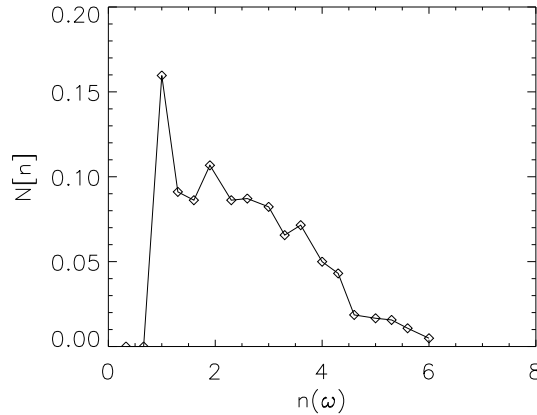
Figure 8. The relative number of orbits with different complexities $n(\omega)$, computed for the same ensemble used to generate Figure 3 b.

Less obvious, however, but also true is that even for a collection of wildly chaotic orbits, where $N[\chi]$ peaks at some intermediate value of χ, $N[n]$ can be a sharply decreasing function of n. This is, *e.g.*, evident from Figure 8, which plots $N[n]$ for the same orbit ensemble used to generate the distribution $N[\chi]$ in Figure 3 b. In this plot, the orbits with $n(\omega) < 2$ are almost all regular or nearly regular, whereas the orbits with $n(\omega) > 2$ are almost all wildly chaotic. The obvious point is that, for $n(\omega) > 2$, the distribution $N[n]$ decreases in a near-uniform fashion, even though the corresponding distribution $N[\chi]$ has a pronounced peak at $\chi \sim 0.06$.

Second order perturbation theory can be expected to work reasonably well only when M_{BH} is relatively small; and, for this reason, comparisons between analytic predictions and numerical computations were only effected for $M_{BH} = 0.4$ and less. Even for such small values, however, subtleties remain. By construction, perturbation theory computes shifts in three basic frequencies which, for $M_{BH} = 0$, reduce to $\omega = a$, b, and c. However, one discovers oftentimes that, even for regular orbits, $M_{BH} > 0$ implies spectra with power at more than three frequencies; and, for fully chaotic orbits, the spectra should, strictly speaking, be continuous (*cf.* Tabor 1989), although most of the power may be concentrated at or near a small number of frequencies. For this reason, identifying the relative error between the analytics and numerical computations requires a concrete prescription to identify what one really means by the 'principal' frequencies for oscillations in the x, y, and z directions. As a practical matter, a principal frequency like ω_x
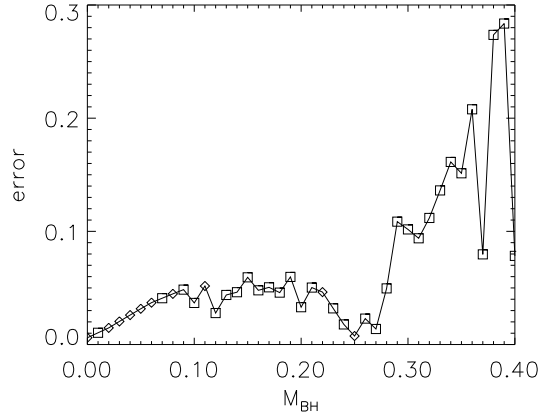
Figure 9. The fractional error between the values of the 'principal' frequency ω_x computed numerically and calculated analytically for a single orbit with $E = 1.0$ evolved in the potential (1) for $t = 2048$ with $a^2 = 1.25$, $b^2 = 1.0$, and $c^2 = 0.75$ for a range of black hole masses $0 \leq M_{BH} \leq 0.4$. Squares denote chaotic orbits, whereas diamonds denote regular or nearly regular orbits.

was extracted by identifying those frequencies in the Fourier spectrum which have at least 70% as much power as that contained in the frequency with maximum power, and then computing a power-weighted average value for these frequencies. A net error between analytics and numerics for a single orbit was derived by averaging over the error associated with the three different frequencies, ω_x, ω_y, and ω_z.

Overall, it was found that, for $M_{BH} < 0.2$ or so, the typical discrepancy between the analytics and numerics is quite small, less than or of order 5%. However, as illustrated in Figure 9, which exhibits the error for ω_x for a single representative orbit, the typical errors become substantially larger for $M_{BH} > 0.2$ or so. One might suppose that analytic predictions of the 'principal frequencies' for chaotic orbits would tend to be much worse than for regular orbits, and that the abrupt increase in relative error for $M_{BH} > 0.25$ reflects the onset of chaos. This, however, is not the whole story. For this initial condition, almost all the orbits with $M_{BH} > 0.08$ are obviously chaotic, but the fractional errors are all less than 0.06 for $M_{BH} < 0.3$.

Nevertheless, it is apparent that, for fixed value of M_{BH}, the typical error grows systematically with increasing complexity, which is hardly surprising in light of the fact that, for large complexity, the 'principal' frequency really involves an average over several different frequencies. This is, *e.g.*, evident in the first panel of Figure 10, which exhibits the average error as a function of $n(\omega)$ for the same orbit ensemble
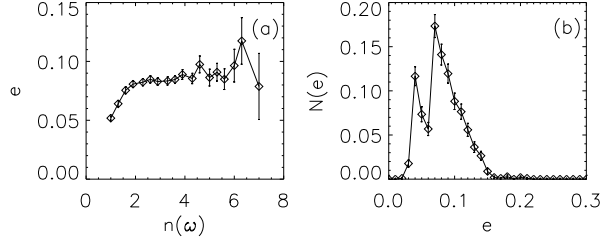
Figure 10. (a) The average fractional error as a function of $n(\omega)$, the number of frequencies with amplitude greater than 0.7 times the frequency with peak power for the orbit ensemble used to generate Figure 7. The error bars reflect the spread of values observed for orbits with the same $n(\omega)$. (b) The relative fraction of the orbits in the ensemble with different fractional errors.

used to generate Figure 7. That perturbation theory is more successful overall in accounting for regular and nearly regular orbit segments than for wildly chaotic segments is evident from the second panel in Figure 10, which plots $N[e]$, the distribution of relative errors. That the distribution is sharply bimodal is consistent with the fact that, as regards the success of perturbation theory, the orbits divide into two distinct populations, one, comprised mostly of regular orbits, for which perturbation theory is quite reliable, and another, comprised mostly of wildly chaotic orbits, for which perturbation theory works somewhat less well.

But precisely *why* does the observed chaos actually arise? A detailed examination of the local stability of individual orbits provides a simple and compelling answer. When an orbit is far from the center, the central mass M_{BH} has only a comparatively minimal effect and the orbit is nearly regular. However, when the orbit comes too close to the center and M_{BH} contributes significantly to the total potential experienced by the orbit, the combination of the incompatible symmetries leads to a resonance overlap and a significant exponential instability. This is, *e.g.*, illustrated in Figure 11, which exhibits a representative piece of a wildly chaotic orbit segment with $E = 0.75$ evolved in the potential (1) with $a^2 = 1.25$, $b^2 = 1.0$, $c^2 = 0.75$, and $M_{BH} = 0.15$. Here the solid curve in the top panel displays the phase space separation $|\delta Z(t)|$ between the original orbit and a perturbed orbit displaced originally by a distance $|\delta Z| = 10^{-8}$ and renormalised in the usual way (*cf.* Lichtenberg and Lieberman 1992) at intervals $\delta t = 12.0$. The dashed curve shows an analogous plot of $|\delta Z|$ for a regular orbit. The bottom panel exhibits $r(t)$, the distance from the origin (solid curve), and $|V_p| = M_{BH}/\sqrt{r^2 + \epsilon^2}$, the magnitude of the central mass perturbation. The obvious point is that most of the time the perturbed
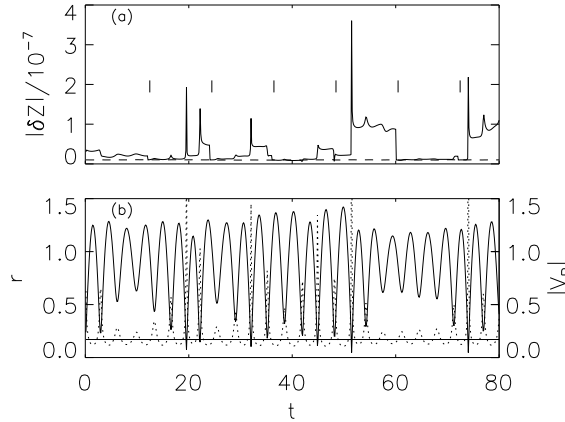
Figure 11. (a) The solid curve shows $|\delta Z|(t)$, the magnitude of the phase space distance between a perturbed and unperturbed chaotic orbit evolved in the potential (1) with $a^2 = 1.25$, $b^2 = 1.0$, $c^2 = 0.75$, $M_{BH} = 0.15$, and $E = 0.75$. For comparison, the dashed line shows $|\delta Z|$ for a regular orbit. The orbit was renormalised at intervals $\delta t = 12.0$ at points indicated by vertical stripes in the plot. (b) The solid curve shows $r(t)$, the distance from the origin, for the same orbit at the same times. The dotted line shows the magnitude of the perturbation, $|V_p| = M_{BH}/\sqrt{r^2 + \epsilon^2}$. The vertical line corresponds to a value $r = 0.17$, for which $|V_p| \approx 0.88$.

and unperturbed orbit remain very close together, with little if any systematic exponential divergence; but that when $r < 0.17$ or so, so that $|V_p|$ becomes as large as ~ 0.88, the two orbits tend to diverge significantly.

In this context, it should be noted that, even for the orbits which have been characterised as 'wildly chaotic,' the computed Lyapunov exponents are comparatively small when expressed in units of t_D. For 'generic' chaotic potentials, one discovers typically that the largest Lyapunov exponent typically assumes a value $\sim 0.5t_D^{-1} - 1.0t_D^{-1}$ which, for $t_D \sim 2 - 3$, implies values of χ in excess of 0.2 or so. However, only for very large central masses, $M_{BH} > 0.3$ or so, did any of the computed orbit segments have values of χ as large as 0.2. Even the so-called wildly chaotic orbits tend to be comparatively regular most of the time, the observed chaos resulting from those comparatively rare intervals when the orbits come comparatively close to the central mass.

4. Discussion

The stickiness manifested by chaotic orbits in the potential explored in this paper is strikingly reminiscent of what has been observed for

the triaxial analogues of the Dehnen potentials (*cf.* Merritt and Valluri 1996, Siopis and Kandrup 2000), especially for those orbits which, in the absence of the cusp and/or black hole, would correspond to box orbits. Introducing a cusp and/or a supermassive black hole into an otherwise smooth triaxial potential can generate a considerable amount of chaos, but individual orbit segments can be very nearly regular for very long times. Stickiness appears to be a more important phenomenon in cuspy triaxial potentials, both with and without a central black hole, than in many other chaotic three-dimensional potentials.

The numerical experiments described in Section 2 – especially the fact that quantities like the relative measure of chaotic, as opposed to regular, orbits can manifest a nontrivial dependence on both M_{BH} and axis ratio – suggests strongly that the chaos associated with this potential results from a resonance overlap between the natural frequencies of the unperturbed oscillator and the natural frequencies of the central black hole. An examination of the local stability of individual orbits indicates that, for intermediate black hole masses, the orbits are only very unstable when they are sufficiently close to the black hole that $|V_o|$ and $|V_p|$ become comparable in magnitude. The computations for this simple potential thus corroborate the conclusions of Valluri and Merritt (1998) based on a detailed investigation of the spectral properties of orbits in the triaxial Dehnen potentials. However, it is also evident that the chaos arises in response to a combination of incompatible symmetries: the Plummer and oscillator potentials are each integrable separately but, when combined with comparable magnitudes, can yield strongly chaotic behaviour.

The simplicity of the potential (1) was important because it made possible the analytic calculations described in Section 3. However, this potential *is* artificial in the sense that, for fixed energy E, every orbit unperturbed by a central black hole has the same natural frequencies, a fact that renders the conclusions of the paper anomalous in two significant respects: (1) As is clear, *e.g.*, from Figures 2 and 3, as M_{BH} increases there is an extremely abrupt transition from a phase space hypersurface with essentially no chaos to a phase space that is almost completely chaotic. If the harmonic oscillator component of the potential is replaced by an anharmonic oscillator, *e.g.*, by allowing for quartic corrections, the natural frequencies of different unperturbed orbits with the same energy are no longer identical, and one would anticipate the transition from little chaos to much chaos to become more gradual. (2) If the oscillator is made anharmonic, the nontrivial structures exhibited by $n(M_{BH})$ and $n(\Delta)$ might also be expected to disappear. Because an ensemble of fixed energy now involves unperturbed orbits with different frequencies, a plot of $n(M_{BH})$ can be understood as
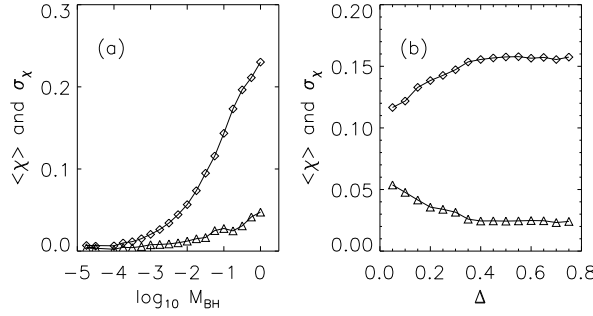
Figure 12. (a) The average short time Lyapunov exponents, $\langle\chi\rangle$ (diamonds), and the associated dispersions, σ_χ (triangles), for representative ensembles with $\epsilon = 10^{-2}$, $E = 1.0$, and $a^2 : b^2 : c^2 = 1.25 : 1.00 : 0.75$ evolved in the anisotropic potential (3) with $\alpha = 1.0$ and variable M_{BH}. (b) The average short time Lyapunov exponents, $\langle\chi\rangle$ (diamonds), and the associated dispersions, σ_χ (triangles), for representative ensembles with $\epsilon = 10^{-2}$, $E = 1.0$, $M_{BH} = 0.1$, and $a^2 : b^2 : c^2 = 1+\Delta : 1 : 1-\Delta$ for variable Δ.

involving a nontrivial superposition of orbits with different unperturbed frequencies.

These expectations were confirmed by repeating the computations described in this paper for orbits in the generalised potential

$$V(x, y, z) = \frac{1}{2}(a^2 x^2 + b^2 y^2 + c^2 z^2)$$

$$+\frac{\alpha}{4}(a^2 x^4 + b^2 y^4 + c^2 z^4) - \frac{M_{BH}}{\sqrt{r^2 + \epsilon^2}}, \qquad (3)$$

for a variety of different values of α. Data for the representative value $\alpha = 1$ are exhibited in Figure 12. Here the first panel exhibits the mean $\langle\chi\rangle$ and dispersion σ_χ for 2000 orbit ensembles with $E = 1.0$, $a^2 = 1.25$, $b^2 = 1.0$, $c^2 = 0.75$ and $\epsilon^2 = 10^{-4}$ for different values of M_{BH}. The second panel exhibits the same quantities for ensembles with $E = 1.0$, $M_{BH} = 0.1$, $\epsilon^2 = 10^{-4}$, and $a^2 : b^2 : c^2 = 1 + \Delta : 1 : 1 - \Delta$ for different values of Δ. It is evident from panel (a) that that the transition to chaos is more gradual than was observed in the harmonic potential. Moreover, only for black hole masses somewhat smaller than $M_{BH} = 10^{-4}$ do all the orbits seem completely regular. And similarly, it is clear that $\langle\chi\rangle$ and σ_χ vary smoothly with M_{BH} and Δ, the resonant behaviour observed for $\alpha = 0$ having washed out because the ensembles now involve unperturbed orbits with a variety of frequencies.

Appendix

The Hamiltonian appropriate for motion in the potential (1) can be written in the form $H = H_0 + H_1$, where

$$H_0 = \frac{1}{2}(P_x^2 + P_y^2 + P_z^2) + \frac{1}{2}(A_x^2 Q_x^2 + A_y^2 Q_y^2 + A_z^2 Q_z^2) \qquad (4)$$

is integrable and

$$H_1 = -\frac{M_{BH}}{\sqrt{Q_x^2 + Q_y^2 + Q_z^2 + \epsilon^2}} \qquad (5)$$

may be viewed as a perturbation that breaks integrability. Because the integrable component H_0 is separable, it is easy to compute the generating functional $W(Q_1, J_1, Q_2, J_2, Q_3, J_3)$, which can be written as

$$W = \sum_{i=1}^{3} \frac{1}{2} Q_i \sqrt{2J_i - A_i^2 Q_i^2} + \frac{J_i}{A_i} \sin^{-1}\left(\frac{A_i x_i}{\sqrt{2J_i}}\right) \qquad (6)$$

where J_i denote the actions and the index i ranges over x, y, and z. Given W, it is easy to relate the original canonical variables to the actions J_i and a corresponding set of angles θ_i, in terms of which the Hamiltonian reduces to $H = H_0 + H_1$, where

$$H_0 = J_1 + J_2 + J_3 \qquad (7)$$

and

$$H_1 = -M_{BH} \times$$

$$\left[\frac{2J_1}{A_1^2} \sin^2 A_1\theta_1 + \frac{2J_2}{A_2^2} \sin^2 A_2\theta_2 + \frac{2J_3}{A_3^2} \sin^2 A_3\theta_3 + \epsilon^2\right]^{-1/2}. \qquad (8)$$

At this stage, one needs to perform a triple integral, averaging each of the three angles over the range $0 < \theta < 2\pi$. Unfortunately, however, this is difficult to do in closed form. Nevertheless, one can proceed perturbatively by expanding H_1 in a Taylor series around some point $(\theta_1, \theta_2, \theta_3) = (q_1, q_2, a_3)$. The result of such a computation is that the perturbed frequencies ω_i satisfy

$$\frac{\omega_i}{A_i} = 1 + \frac{\partial}{\partial J_i}\left[H_1(M_{BH}, q_1, q_2, q_3, J_1, J_2, J_3) + \right.$$

$$\left. + \sum_{j=1}^{3}\left(\frac{\partial H_1}{\partial q_j}\right)(\pi - q_j)\right.$$

$$+ \; \frac{1}{2} \sum_{j=1}^{3} \left(\frac{\partial^2 H_1}{\partial q_j^2} \right) \left(\frac{4}{3} \pi^2 - 2\pi q_j + q_j^2 \right)$$

$$+ \; \sum_{j<k=1}^{3} \left(\frac{\partial^2 H_1}{\partial q_j \partial q_k} \right) [(\pi - q_j)(\pi - q_k)] \Bigg]. \tag{9}$$

It is natural to choose the q_i's at or near values for which $A_i qi = \pm\pi/2$, for which values the magnitude of H_1 is minimised.

Acknowledgements

References

V. I. Arnold, *Russian Math. Surveys* 18: 85, 1964

J. Binney, *Comments Astrophys.* 8: 27, 1978

G. Contopoulos, *Astron. J.* 76: 147, 1971

W. Dehnen, *Mon. Not. R. Astr. Soc.* 265: 250, 1993

T. Fridman and D. Merritt, *Astro. J.* 114: 1479, 1997

P. Grassberger, R. Badii, R., and A. Politi, *J. Stat. Phys.* 51: 135, 1988

H. E. Kandrup, B. L. Eckstein, and B. O. Bradley, *Astron. Astrophys.* 320: 65, 1997

H. E. Kandrup and M. E. Mahon, *Phys. Rev. E* 49: 3735, 1994

D. E. Kaufmann and G. Contopoulos, *Astron. Astrophys.* 309: 381, 1996

J. Kormendy and R. Bender, *Astrophys. J. Lett.* 464: 119, 1996

J. Kormendy and D. Richstone, *Ann. Rev. Astron. Astrophys.* 33: 581, 1995

T. Lauer, *et al*, *Astron. J.* 110: 2622, 1995

A. J. Lichtenberg and M. A. Lieberman, *Regular and Chaotic Orbits*, Berlin, 1992. Springer

D. Merritt and T. Fridman, *Astrophys. J.* 460: 136, 1996

D. Merritt and M. Valluri, *Astrophys. J.* 471: 82, 1996

D. Merritt and M. Valluri, *Astron. J.* 118: 1177, 1999

P. A. Patsis, E. Athanassoula, and A. C. Quillen, *Astrphys. J.* 483: 731, 1997

M. Schwarzschild, *Astrophys. J.* 409: 563, 1993

C. Siopis, B. L. Eckstein, and H. E. Kandrup, *Ann. N. Y. Acad. Sci.* 867: 41, 1998

C. Siopis and H. E. Kandrup, *Mon. Not. R. Astr. Soc.* 319: 43, 2000

S. Sridhar and J. Touma, *Mon. Not. R. Astr. Soc.* 287: L1, 1996

S. Sridhar and J. Touma, *Mon. Not. R. Astr. Soc.* 292: 657, 1997

M. Tabor, *Chaos and Integrability in Nonlinear Dynamics*, New York, 1989. Wiley.

S. Udry and D. Pfenniger, *Astron. Astrophys.* 198: 135, 1988

M. Valluri and D. Merritt, *Astrophys. J.* 506: 686, 1998

H. Wozniak, In V. G. Gurzadyan and D. Pfenniger, editors *Ergodic Concepts in Stellar Dynamics*, Berlin, 1993. Springer.